IOPscience iopscience.iop.org

Home Search Collections Journals About Contact us My IOPscience

Raman studies of the ferroelectric phase transitions in $(CH_3NH_3)_5Bi_2Cl_{11}$ (MAPCB). I. The internal vibrations of the methylammonium cation

This article has been downloaded from IOPscience. Please scroll down to see the full text article.

1992 J. Phys.: Condens. Matter 4 2985

(http://iopscience.iop.org/0953-8984/4/11/023)

View the table of contents for this issue, or go to the journal homepage for more

Download details:
IP Address: 171.66.16.159
The article was downloaded on 12/05/2010 at 11:32

Please note that terms and conditions apply.

J. Phys.: Condens. Matter 4 (1992) 2985–2999. Printed in the UK

Raman studies of the ferroelectric phase transitions in $(CH_3NH_3)_5Bi_2Cl_{11}$ (MAPCB): I. The internal vibrations of the methylammonium cation

P Carpentier†, J Lefebvre† and R Jakubas‡

† Laboratoire de Dynamique et Structures des Matériaux Moléculaires (UA 801), UFR de Physique, Université de Lille I, 59655 Villeneuve d'Ascq Cédex, France

‡ Institute of Chemistry, University of Wrocław, PL 50383 Wrocław, Poland

Received 3 June 1991, in final form 23 September 1991

Abstract. The Raman spectra of $(CH_3NH_3)_5Bi_2Cl_{11}$ in the range of internal frequency modes of the $(CH_3NH_3)^+$ cation (750–1700, 2700–3500 cm^{-1}) have been recorded in the three phases and at room temperature for the partially deuterated (CD_3NH_3) compound. The CH_3 (or CD_3) and NH_3^+ bands of the spectra have been identified and compared with Raman results available for other methylammonium crystals. The temperature dependences of these internal modes were measured in the range 100–360 K and their temperature behaviour has been explained by a model of linear and quadratic pseudospin–phonon interactions.

1. Introduction

The alkylammonium halogenobismuthate (III) crystals of general formula $(CH_3NH_3)_5Bi_2X_{11}$ (X = Cl, Br) evoke considerable interest in connection with the appearance of ferroelectric properties. Since the discovery of ferroelectricity in this family of compounds [1, 2], many experimental investigations of these crystals, $(CH_3NH_3)_5Bi_2Cl_{11}$ (MAPCB) and $(CH_3NH_3)_5Bi_2Br_{11}$ (MAPBB), have been reported.

Crystal structures have been studied in the paraelectric (Cl and Br analogue) and ferroelectric phases (Cl) [3, 4]. Further, various properties such as dielectric constants [5, 6], pressure dependence of the dielectric constants (Br) [7], pyroelectricity (Cl, Br) [8, 9], dielectric dispersion $\varepsilon^*(\omega)$ (Cl, Br) [10, 11], thermal expansion (Br) [12], electro-optic constants (Pockels effect, Cl, Br) [13, 14] and birefringence (Cl, Br) [15, 16] have been measured.

The motion of methylammonium ions in the crystals has been studied by means of ^1H NMR experiments (Br) [17] and infrared and Raman scatterings (Br) [18, 19]. The isomorphous nature of the Cl and Br compounds is reflected in the sequence of phase transitions (PT) observed:

	Second-order PT		Second order PT	
	T_{C_2}		T_{C_1}	
		orthorhombic		orthorhombic
?		$Pca2_1$		Pcab
	77 (Br)		311.5 (Br)	
	170 (Cl)		307.0 (Cl)	
polar phase		ferroelectric		paraelectric
(III)		(II)		(I)

0953-8984/92/112985 + 15 $04.50 © 1992 IOP Publishing Ltd

A transition mechanism for the high-temperature ferro–paraelectric transformation for the chlorine analogue has been proposed by Lefebvre *et al* [3], by comparing the ordering of the methylammonium cations in the ferroelectric phase at 294 K and in the paraelectric phase at 349 K. Above T_{C_1}, three of the five $(CH_3NH_3)^+$ cations are disordered. When the I–II PT is crossed, only one type of methylammonium cations becomes ordered, forming a new N–H $\cdots$ Cl hydrogen bond along the polar direction c, whereas the remaining $(CH_3NH_3)^+$ cations are still disordered until the lower II–III PT. We believe that the latter type of cations may contribute to the ferro–polar PT at 170 K.

The 'order–disorder' mechanism of the I–II PT evident from our x-ray studies has recently been corroborated by the dielectric dispersion studies of $\varepsilon^*(\omega)$ in the microwave region, showing the critical slowing down for both MAPBB [10] and MAPCB [11] at T_{C_1}. Very recently, the same mechanism was suggested by a dielectric dispersion study on MAPBB in the vicinity of the III–II PT [20].

Preliminary Raman scattering measurements on single crystals of MAPBB in the lattice region [18] have not revealed any significant changes for the lattice modes close to T_{C_1}, but the lack of a soft mode was in agreement with the results for the dielectric dispersion $\varepsilon^*(\omega)$. Recent Raman studies on the 166 cm^{-1} mode (probably the librational mode of the $CH_3NH_3^+$ cation) in powdered samples of MAPBB have shown a temperature dependence close to $T_{C_1} = 311$ K due to order–disorder processes [19].

The present paper is devoted to Raman studies of the internal modes of the fully hydrogenous $(CH_3NH_3)^+$ and partially deuterated $(CD_3NH_3)^+$ methylammonium cations of the chlorine analogue MAPCB in the temperature range 100–360 K.

2. Experimental procedure

The $(CH_3NH_3)_5Bi_2Cl_{11}$ crystals were obtained by reaction of $(BiO)_2CO_3$ and CH_3NH_2 in a solution of HCl. The single crystals were grown from a dilute solution by slow evaporation at 293 K. To obtain $(CD_3NH_3)_5Bi_2Cl_{11}$, the same synthesis was carried out using CD_3NH_2. The sample of MAPCB used for these experiments had a size of about $3 \times 3 \times 2$ mm^3. Its faces were perpendicular to the three crystallographic directions a, b and c.

The Raman spectra were excited with 488 nm radiation from a Spectra Physics ionized argon laser. The Stokes components, scattered at 90° to the incident beam direction, were analysed with a Coderg T800 triple monochromator. The spectral resolution was of order 1.5 cm^{-1}. Photon counting and a Dilor data acquisition system coupled with an Apple IIe microcomputer and a Micro-Vax II computer allowed for recording and numerical simulation of experimental spectra. Raman spectra were recorded in the range of the internal frequency modes of the methylammonium cation, 750–1700 cm^{-1} and 2700–3500 cm^{-1}. An additional spectrum, from 1900–2500 cm^{-1}, was recorded for the partially deuterated compound.

The sample was mounted in a goniometer head, permitting precise orientation of the crystal with respect to the directions of the incident and scattered beams. The estimated misalignments were less than 1°. Low- and high-temperature measurements were made using specially designed systems, in which a stream of cool or hot gaseous nitrogen was blown onto the sample.

3. Analysis of normal modes

A free methylammonium cation, of C_{3v} symmetry, has 18 internal modes. The decomposition into irreducible representations is as follows: $5\,A_1 + 1\,A_2 + 6\,E$, and, with degenerate E modes, there are twelve different frequencies. Both the para- and ferroelectric phases have 20 methylammonium cations in the unit cell. In the ferroelectric phase with C_{2v} as point group, all the $(CH_3NH_3)^+$ cations are in the general position. In the paraelectric phase, where the point group is D_{2h}, 16 $(CH_3NH_3)^+$ cations are in the general position. Eight of them are ordered and the other eight are disordered; the remaining four are disordered and lie statistically about an inversion centre. Table 1 gives correlations between the symmetry modes of the free methylammonium cation and the symmetry modes of the C_{2v} and D_{2h} point groups.

Table 1. Correlation table of the internal normal modes of the methylammonium cation in MAPCB (*a*) (R: Raman active mode; IR: infrared active mode) and compatibility between the symmetry modes of C_{2v} and D_{2h} (*b*). For a mode of E symmetry in the free cation (C_{3v}), the mode number in phases II and I is twice the mode number of the A_1 or A_2 symmetries in (*a*).

Free $(CH_3NH_3)^+$ C_{3v}	Phase II C_{2v}	Free $(CH_3NH_3)^+$ C_{3v}	Phase I D_{2h}
(*a*)			
A_1 or A_2	$5\,A_1$ (R, IR) $5\,A_2$ (R) $5\,B_1$ (R, IR) $5\,B_2$ (R, IR)	A_1 or A_2	$2\,A_g$ (R) $2\,B_{1g}$ (R) $2\,B_{2g}$ (R) $2\,B_{3g}$ (R) $3\,A_u$ $3\,B_{1u}$ (IR) $3\,B_{2u}$ (IR) $3\,B_{3u}$ (IR)
(*b*)	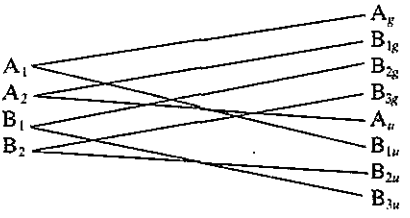		

For the Raman-active irreducible representations of the C_{2v} and D_{2h} point groups, the polarizability tensors have the form

$$A_1(z), A_g: \begin{bmatrix} a & . & . \\ . & b & . \\ . & . & c \end{bmatrix} \qquad A_2, B_{1g}: \begin{bmatrix} . & d & . \\ d & . & . \\ . & . & . \end{bmatrix}$$

$$B_1(x), B_{2g}: \begin{bmatrix} . & . & e \\ . & . & . \\ e & . & . \end{bmatrix} \qquad B_2(y), B_{3g}: \begin{bmatrix} . & . & . \\ . & . & f \\ . & f & . \end{bmatrix}.$$

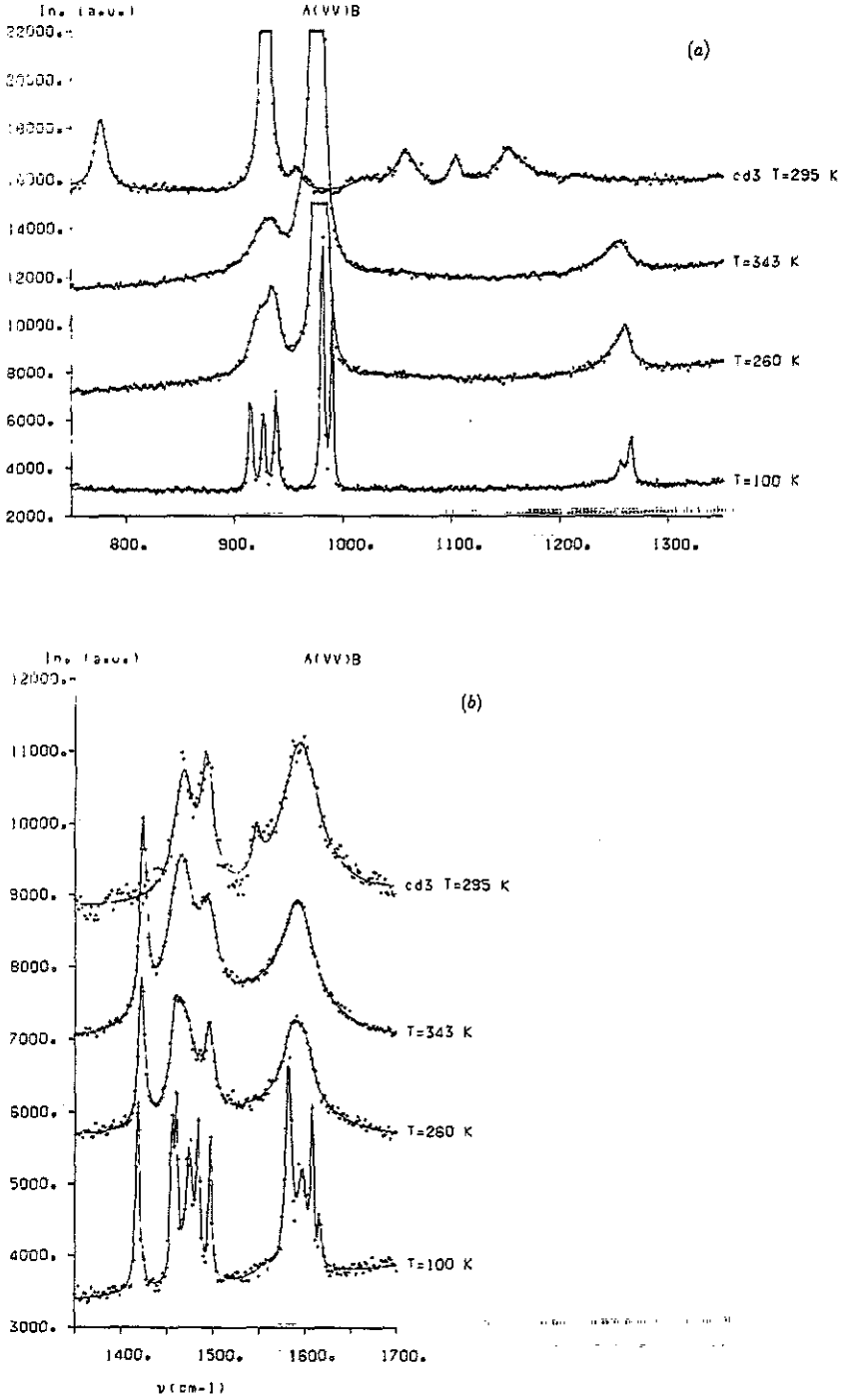

Figure 1. Raman spectra of fully protonated (T = 100, 260 and 343 K) and partially deuterated (T = 295 K) MAPCB. ×, are experimental points; ———, calculated intensity using an appropriate number of oscillators (*a*) from 750 to 1350 cm^{-1}, (*b*) from 1350 to 1700 cm^{-1}, (*c*) from 2700 to 3500 cm^{-1}, and (*d*) from 1900 to 2500 cm^{-1} (for the partially deuterated compound only).

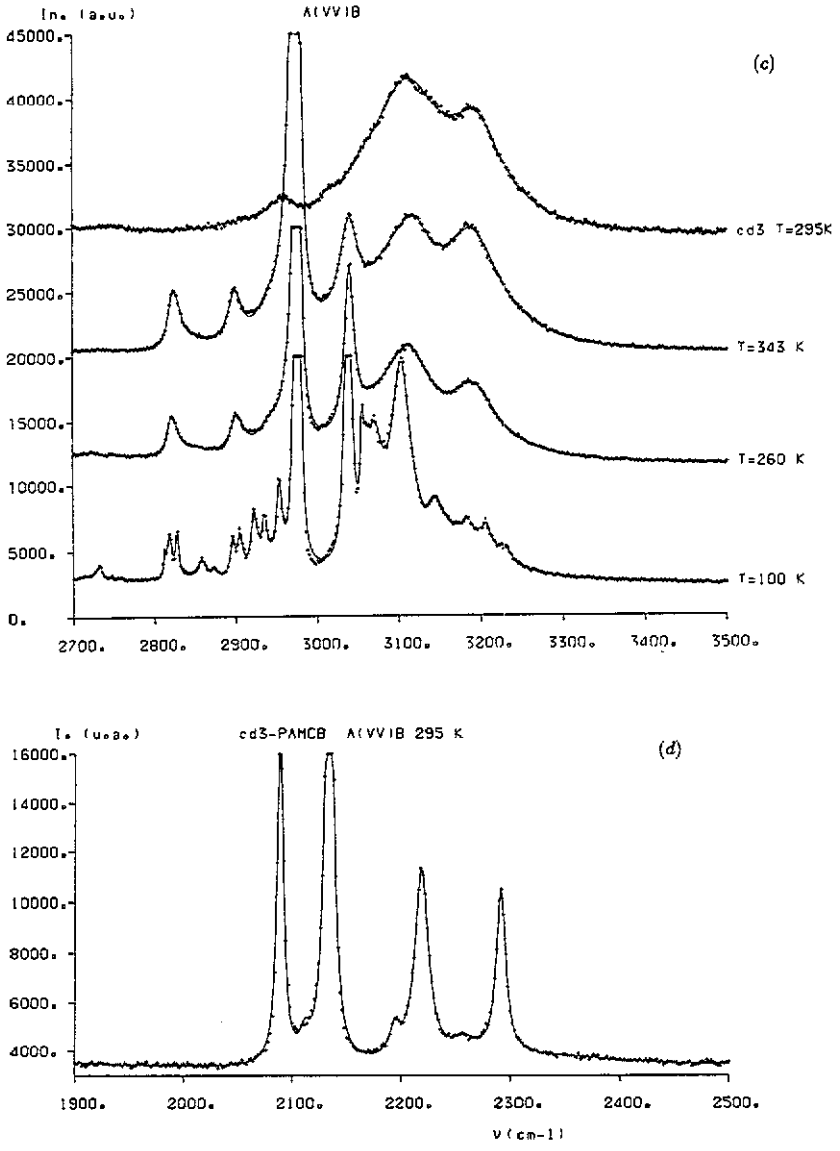

Figure 1. Continued.

With the *c* crystallographic direction perpendicular to the scattering plane, and by changing the polarization of the incident and scattering beams, it was possible to find the modes of the four Raman-active symmetries.

4. Interpretation of spectra

Polarized Raman spectra were recorded at room temperature (phase II) and at 343 K (phase I), in the frequency region of the $(CH_3NH_3)^+$ internal modes. In all four spectra,

Table 2. Raman frequencies (in cm^{-1}) of the internal modes, for MAPCB, of the methylammonium cation $(CH_3NH_3)^+$ in the three phases and $(CD_3NH_3)^+$ at room temperature.

Phase III $T = 100$ K	$(CH_3NH_3)^+$ Phase II $T = 260$ K	Phase I $T = 343$ K	$(CD_3NH_3)^+$ $T = 295$ K	Assignment
3230.0	—	—	—	
3207.0	—	—	—	
3184.0	—	—	—	
3179.0	3192.0	3191.0	3198.0	ν_7: asym. NH_3 stretch
3146.0	—	—	—	
3103.3	3112.7	3118.3	3110.0	
3070.1	3074.0	3087.0	3054.0	ν_1: sym. NH_3 stretch
—	—	—	3016.0	
3040.1	3040.3	3040.0	2292.0	ν_8: asym. CH_3 stretch
3034.4	—	—	—	
2979.1	2978.6	2978.5	—	ν_2: sym. CH_3 stretch
2974.5	2974 1	2972.0	2134.0	
1608.6	1602.0	—	—	
1597.4	—	—	—	ν_9: asym. NH_3 bend
1582.9	1588.2	1593.8	1596	
1497.4	1496.8	1495.1	1494.0	
1483.9	—	—	—	ν_3: sym. NH_3 bend
1474.2	1479.7	1465.0	1467.0	
1459.1	—	—	—	ν_{10}: asym. CH_3 bend
1455.1	1459.0	—	1058.0	
1418.5	1422.4	1424.0	1104.0	ν_4: sym. CH_3 bend
1265.4	1260.5	1254.8	1158.0	
1256.4	1250.0	1236.0	1151.0	ν_{11}: rocking
1240.0	—	—	—	
989.8	982.8	979.3	—	ν_5: CN stretch
981.1	977.1	975.6	929.0	
938.6	936.6	—	—	
926.8	—	—	—	ν_{12}: rocking
914.9	922.3	930.3	777.0	

ν_1 to ν_5 are A_1 modes of the C_{3v} symmetry; ν_7 to ν_{12} are E modes.

the same bands appear with a shift less than 1 cm^{-1}, and this explains why we decided to focus our study on the A_1 or A_g modes only. As the A_1 modes are polar in the ferroelectric phase, some Raman spectra were recorded at room temperature using the back-scattering method and with the *a* axis vertical. Possible LO–TO splittings appeared negligible.

Figure 1 shows the Raman spectra of the $(CH_3NH_3)^+$ internal modes at 343 K (phase I), 260 K (phase II), 100 K (phase III) and for $(CD_3NH_3)^+$ at room temperature. Table 2 gathers the measured frequencies in MAPCB. A tentative assignment for these modes is also given in this table, made with respect to the symmetry modes of the free $(CH_3NH_3)^+$

cation with C_{3v} symmetry [21]. The assignment is based on comparison between experimental and calculated frequencies using the valence force field model [22].

The torsional A_2 modes of the free cation with frequencies expected at about 400 cm^{-1} were not measured.

The effect of the crystal field leads to the splitting of the symmetry modes of the free methylammonium cation. However, the number of splitting components observed for all measured bands never corresponds with the predictions of group theory. There are at least two reasons for this disagreement: (i) the effect of the crystal field for some bands is too small and hence two or more modes can be superposed; (ii) the intensity of the mode is very low. The last argument is especially relevant for the ferroelectric phase: an A_1 mode of this phase comes from either a Raman active A_g mode or a Raman inactive B_{1u} mode of the paraelectric phase (table 1). As will be seen in the next section, only a few bands appear when the transition is crossed and most of the B_{1u} modes have a very low intensity in the ferroelectric phase.

Important splittings appear only for the NH_3 group modes. This is the case for the asymmetric NH_3 stretching mode (ν_7 mode) where two components range from about 3112 to 3192 cm^{-1} in phases I, II and for $(CD_3NH_3)^+$ and six components appear in phase III in the range 3103–3230 cm^{-1}. Three other modes: the symmetric NH_3 stretching (ν_1 mode), the symmetric and asymmetric NH_3 bendings (ν_3 and ν_9 modes, respectively) also present an important splitting of order 20–40 cm^{-1} between their two components. These splittings can be explained by the existence in MAPCB of N–H $\cdots$ Cl hydrogen bonds for some hydrogen atoms of the NH_3 groups [3]. These values have been compared with the frequencies measured by Raman and infrared spectroscopies in $(CH_3NH_3)_2CdCl_4$ [23] and $(NH_3CH_3)Cl$ [21]. In the former compound, where all the hydrogen atoms of the NH_3 groups are involved in N–H $\cdots$ Cl hydrogen bonds, the frequencies of the ν_7, ν_1, ν_9 and ν_3 modes, at 3175, 3105, 1594 and 1496 cm^{-1} respectively, are close to the high-frequency component of each mode in MAPCB. For the latter compound in its α-phase, the hydrogen bonds are very weak and the frequencies of the four modes discussed are 3086, 2980, 1556 and 1530 cm^{-1} (i.e. they are comparable (except ν_3) to our lower frequency components). The four additional NH_3 stretching modes in phase III correspond to new and different hydrogen bonds in the low-temperature lattice.

In contrast, in the case of the modes corresponding to displacements of the CH_3 group atoms only (ν_2, ν_4, ν_8 and ν_{10} modes), the splittings are smaller (about 5 cm^{-1}), except ν_4, where only one component has been observed. The frequency values for these four modes of the fully hydrogenated MAPCB are almost the same as for $(CH_3NH_3)_2CdCl_4$ and $(CH_3NH_3)Cl$. For the C–N stretching mode (ν_5), there are two components with a small splitting (about 5 cm^{-1}) and their frequencies are in agreement with those of the two other compounds.

The two rocking modes (ν_{11} and ν_{12}) are also split into two components (three components in phase III). According to Sundius and Meinander [22], these two modes are strongly coupled and the splitting of order 15 cm^{-1} for both modes is also due to hydrogen bonding.

The isotopic effect on the band positions in the partially deuterated methylammonium cation $(CD_3NH_3)^+$ is easily visible and allows us to assign the different bands more precisely. In the case of the modes corresponding to the displacements of the NH_3 group atoms, the frequencies for the two compounds are almost the same. Considering the modes where the atoms of the CH_3 group are involved, the frequency ratios (ν_D/ν_H) between the corresponding modes of the two compounds are 0.712, 0.775,

0.754 and 0.725 for the ν_2, ν_4, ν_8 and ν_{10} modes, respectively. These are close to the theoretical value of 0.734. The frequency ratio for the C–N stretching mode (ν_5) is 0.950, whereas the theoretical value is 0.955.

Owing to second-order Raman scattering, there are many bands between 2700 and 3000 cm^{-1} in the experimental spectra of both compounds. We have also observed second-order Raman bands between 2000 and 2300 cm^{-1} in the $(CD_3NH_3)^+$ compound. In table 3, the proposed assignment of these lines is given.

The most interesting point of this second-order Raman scattering study concerns the overtones of the two CH_3 bending modes ($2\nu_4$ and $2\nu_{10}$). As for $(CH_3NH_3)Cl$ [21], the intensities of these bands are enhanced by Fermi resonance with the fundamental ν_2 mode. Discussion of the second-order Raman scattering in fully hydrogenated MAPCB is much more complicated than for the case of $(CH_3NH_3)Cl$ due to splitting of the ν_2, $2\nu_4$ and $2\nu_{10}$ bands into two components in phase III. The methyl bending fundamental ν_4 and ν_{10} frequencies, their overtones ($2\nu_4$) and ($2\nu_{10}$), the two symmetric stretching ν_2 components as well as the ($2\times\nu_i - 2\nu_i$) shifts and ($\nu_2 - 2\nu_i$) differences are collected in table 3(*a*). We indicate by $2\times\nu_i$ the frequency of the *i*th fundamental multiplied by two and by $2\nu_i$ the measured overtone frequency of the *i*th mode. The correspondence between ν_2 and $2\nu_4$ has been made by connecting the lower frequency ν_2 and $2\nu_4$ components and the higher ones. With this procedure, the two ($\nu_2 - 2\nu_4$) differences are almost equal and the first shifts are higher than the second, when approximately the same values are expected. In fact, some additional couplings can occur between these different components. In phase III, there are two ν_{10} and $2\nu_{10}$ components. Connecting the lower frequency values and the higher ones, one finds the same ($2\times\nu_2 - 2\nu_{10}$)

Table 3. Second-order Raman lines in the internal mode frequency region. (*a*) symmetric bending vibration ν_4 and asymmetric bending vibration ν_{10}; (*b*), other overtones.

Assignment	$(CH_3NH_3)^+$ Phase III T = 100 K	Phase II T = 260 K	Phase I T = 343 K	$(CD_3NH_3)^+$ T = 295 K
(*a*)				
ν_2	2974.5, 2979.1	2974.1, 2978.6	2972.0, 2978.5	2134.0
ν_4	1418.5	1422.4	1424.0	1104.0
($2\nu_4$)	2818.0, 2827.5	2820.1, 2826.8	2822.7, 2829.6	2219.0
$2\times\nu_4 - 2\nu_4$	19.5, 9.5	24.7, 18.0	25.3, 18.4	−11.0
$\nu_2 - 2\nu_4$	156.5, 151.6	154.0, 151.8	149.3, 148.9	−85.0
ν_{10}	1455.1, 1459.9	1459.0	—	1058.0
($2\nu_{10}$)	2895.6, 2904.8	2901.7	2899.9	2089.0
$2\times\nu_{10} - 2\nu_{10}$	14.6 15.0	16.3	—	27.0
$\nu_2 - 2\nu_{10}$	78.9 74.3	72.4 76.9	72.1 78.6	45.0
(*b*)				
$\nu_3^1 + \nu_3^2$	2953.0	2966.0	2960.0	2957.0
$\nu_3 + \nu_{10}$	2922.0	2943.0	2941.0	—
$\nu_9 + \nu_{11}$	2873.0 2858.0	— 2848.0	— 2848.0	— —
$\nu_{10} + \nu_{11}$	2732.0	2726.0	2726.0	2194.0
$\nu_4 + \nu_{11}$	—	—	—	2258.0

shifts and also the same $(\nu_2 - 2\nu_{10})$ differences. Nevertheless, results for MAPCB are comparable to those on methylammonium chloride and the same conclusions can be drawn [21]. In particular, it can be seen from table 3(*a*) that there is a correlation between the $(\nu_2 - 2\nu_i)$ differences and the $(2\times\nu_i - 2\nu_i)$ shifts.

Table 3(*b*) presents the other observed overtones with a tentative assignment.

5. Temperature dependence of the internal modes

As mentioned in the introduction, some methylammonium cations are disordered in phases I and II [3]. This disorder can be described as follows. In the ferroelectric phase (phase II), two non-equivalent $(CH_3NH_3)^+$ cations in the general position can occupy two equilibrium sites with reorientational motions around the C–N bond. The probability of finding a cation in a given site is p (this quantity is different for the two cations). In the paraelectric phase (phase I), the previously disordered cations are still disordered, but they become equivalent (they have the same occupancy probability p). In addition, another methylammonium cation is distributed between its two equilibrium sites generated by the inversion centre. For this cation, the two positions are equivalent and the occupancy probability is 0.5.

The frequencies of the internal modes of the fully hydrogenated compound have been measured in the range 100–360 K. Most of the modes change their frequency dependence with temperature at the transition points T_{C_1} and T_{C_2} The two components of ν_5 shown in figure 2 are the most representative example revealing the predominant changes around the PT points. We focus our attention in a temperature range near T_{C_1} because only the mechanism of the I–II phase transition is known. Three different behaviours are observed for the internal mode frequencies of $(CH_3NH_3)^+$ versus temperature. The frequency of some modes softens at T_{C_1}, as can be seen for the ν_1, ν_7, ν_9 and ν_{12} vibrations corresponding to the motions of the NH_3 group. The frequency hardens for other modes, such as one component of ν_2, ν_3, ν_5 and ν_{11}. Finally, there is another group of modes not affected when the transition is crossed.

In the last 15 years, several formalisms have been developed to explain the temperature dependences of the frequency changes below T_C.

Let us focus our attention on the 'hard' modes in the vicinity of the PT points. The changes in the infrared and Raman spectra induced by PT were analysed in terms of

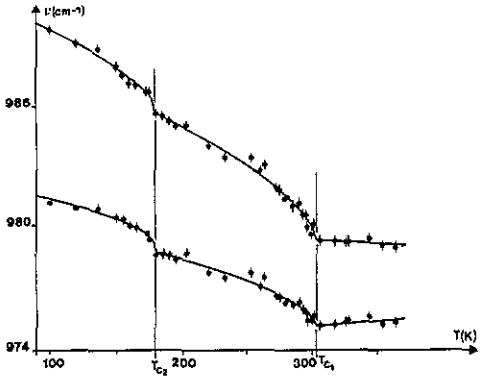

Figure 2. Experimental frequencies versus temperature for the two components of the ν_5 mode. Lines are guidelines for the eyes.

symmetry by Petzelt and Dvořák [24, 25]. They showed that in the case of non-degenerate hard modes (corresponding to our case) the frequency changes very close to T_c are given by the simple relation

$$\Delta\omega \simeq \eta^2$$

where η is the spontaneous value of the order parameter below T_c. Unfortunately, the available experimental data are in good agreement with the Petzelt–Dvořák theory only for crystals exhibiting displacive PTS. On the other hand, it has turned out that in systems with an order–disorder mechanism, the frequency variations of the internal modes have been successfully interpreted by a pseudospin–phonon interaction theory. This theory, used by Matsushita for NH_4Cl and NH_4Br [26] and by Schaack and Winterfeldt for the TGS family [27, 28] agrees satisfactorily with experimental results. Very recently, new Raman results on $(NH_4)_2SO_4$ by Bajpai *et al* agreed with the theoretical expressions of the above model [29].

For this model, pseudospins $S(r_j)$ are introduced to take into account the disorder of the methylammonium cations (r_j locates the cation in the crystal). The Hamiltonian can be written as a sum of three terms:

$$H = H_L + H_S + H_{S,L}. \tag{1}$$

The first term H_L concerns the lattice vibrations. In the harmonic approximation, it can be expressed as

$$H_L = \frac{1}{2}\sum_q \dot{Q}(q)\dot{Q}^*(q) + \omega^2(q)Q(q)Q^*(q) \tag{2}$$

where $Q(q)$ are the phonon normal coordinates, $\dot{Q}(q)$ their derivatives with respect to time and $\omega(q)$ is the frequency of the oscillators. H_S is the interaction energy between the pseudospins. Using an Ising model, it can be expressed as

$$H_S = -\frac{1}{2}\sum_{j,k} J_{jk}S(r_j)S(r_k) = -\frac{1}{2}\sum_q J(q)S(q)S^*(q) \tag{3}$$

where $J(q)$ and $S(q)$ are the Fourier transforms of J_{jk} and $S(r_j)$, respectively; J_{jk} is the interaction energy between pseudospins located at r_j and r_k. The third term of the Hamiltonian, $H_{S,L}$, takes into account the coupling between the pseudospins and the phonons. It can be written as an expansion in powers of the pseudospins and the normal coordinates:

$$H_{S,L} = H_{S,L}^{(1)} + H_{S,L}^{(2)} + H_{S,L}^{(3)} \tag{4}$$

with

$$H_{S,L}^{(1)} = \sum_q V(q)Q(q)S(q) \tag{5}$$

$$H_{S,L}^{(2)} = \sum_{q,q'} V(q,q')Q(q)Q^*(q+q')S(q') \tag{6}$$

$$H_{S,L}^{(3)} = \sum_{q,q',q''} V(q,q',q'')Q(q)Q^*(q+q'+q'')\sum_R [S(r_j)S(r_k)]\,e^{i(q'-q'')R} \tag{7}$$

where $V(q)$, $V(q,q')$ and $V(q,q',q'')$ are coupling constants and $R = r_j - r_k$. The term $H_S + H_{S,L}^{(1)}$ does not result in a frequency shift of optical phonons, because the Ham-

iltonian can be transformed, by eliminating the interaction term, into a 'displaced oscillator' at the unperturbed phonon frequency [30]. First-order perturbation theory shows that $H^{(2)}_{S,L}$ can be written as

$$H^{(2)}_{S,L} = \sum_{q} V(q, 0)Q(q)Q^*(q)S(0). \tag{8}$$

Using the mean field approximation, $S(0)$ can be replaced by its thermal average $\langle S(0)\rangle = \eta(T) \simeq P_S(T)$ where η is the 'order parameter' and P_S the spontaneous polarization. $H^{(3)}_{S,L}$ can be evaluated similarly as $H^{(2)}_{S,L}$ by replacing the pseudospin contribution by its thermal average $\langle S(r_j)S(r_k)\rangle$ and q' and $q'' = 0$. With these assumptions, it can be approximated as

$$H^{(3)}_{S,L} = \sum_{q} V(q, 0, 0)Q(q)Q^*(q) \sum_{R} \langle S(r_j)S(r_k)\rangle. \tag{9}$$

The term $\langle S(r_j)S(r_k)\rangle$ takes into account correlations between pseudospins located at r_j and r_k (the summation over R can be limited to the nearest-neighbour disordered pseudospins). In the paraelectric phase, this term is known to have a temperature dependence like [28]:

$$\langle S(r_j)S(r_k)\rangle \simeq (T - T_{C_1})^{-2\nu} \tag{10}$$

but, in the case of the internal modes of $(CH_3NH_3)^+$, experimental curves show a very small contribution of the quantity in equation (10) and it will be neglected in the following. In the ferroelectric phase, its value lies between the two following extreme cases:

(i) There are no correlations between the two pseudospins, then:

$$\langle S(r_j)S(r_k)\rangle = \langle S(r_j)\rangle\langle S(r_k)\rangle = \langle S(0)\rangle^2 = \eta^2. \tag{11}$$

(ii) All the pseudospins are completely ordered, and in this case

$$\langle S(r_j)S(r_k)\rangle = 1. \tag{12}$$

The intermediate cases are very difficult to estimate, because the numerical values of the interaction potential between the two disordered pseudospins are not known. To simplify, a critical behaviour of $\langle S(r_j)S(r_k)\rangle$ will be assumed in the ferroelectric phase in the vicinity of T_{C_1}, then, a critical exponent is introduced as

$$\sum_{R} \langle S(r_j)S(r_k)\rangle \simeq (T_{C_1} - T)^{\alpha}. \tag{13}$$

The effect of the pseudospin–phonon interactions is to renormalize the square of the phonon frequency as

$$\omega^2_{ph}(q, T) = \omega^2(q) + 2V(q, 0)\eta(T) + 2V(q, 0, 0)\sum_{R} \langle S(r_j)S(r_k)\rangle$$

$$= \omega^2(q) + 2V_0(q)P_S(T) + 2W_0(q)(T_{C_1} - T)^{\alpha}. \tag{14}$$

The spontaneous polarization has been measured from 90 K to T_{C_1} by Mróz and Jakubas [31] and is presented in figure 3. Near the I–II PT, P_S can be approximated, below the transition temperature, by a power law:

$$P_S \simeq (T_{C_1} - T)^{\beta} \tag{15}$$

with $\beta = 0.50$ (until 20 K below T_C), according to the mean field approximation.

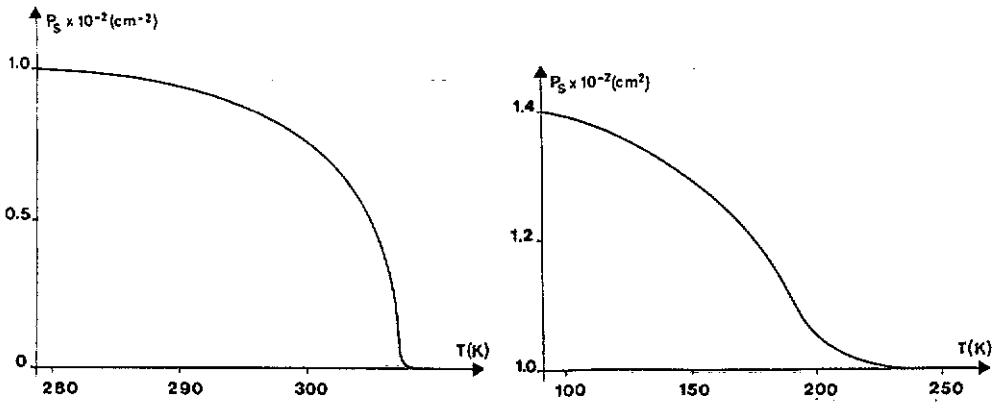

Figure 3 Spontaneous polarization of MAPCB versus temperature.

Taken into account equations (14) and (15), the frequencies $\omega_i(T)$ have been adjusted, in the temperature range 280–360 K, using the following expressions:

$$\begin{aligned} \omega_i^2(T) &= \omega_{0,i}^2 - a_i T + b_i(T_{C_1} - T)^{\beta_i} \qquad \text{for } T < T_{C_1} \\ \omega_i^2(T) &= \omega_{0,i}^2 - a_i T \qquad \text{for } T > T_{C_1} \end{aligned} \tag{16}$$

where $\omega_{0,i}$, a_i, b_i and β_i are adjustable parameters. The term $-a_i T$ takes into account the 'classical' anharmonicity; for internal modes, the slope a_i is generally small or negligible. Only one contribution from the pseudospin–phonon coupling is introduced in equation (16): the temperature dependence of the frequency is assumed to be either linear in the pseudospin coordinates (in this case β_i is 0.5) or quadratic with the value of β_i between 0 and 1. Table 4 gives the values of these calculated critical exponents for the modes with a change in the slope at T_{C_1}. Figure 4 presents experimental points and calculated frequencies with the best sets of parameters obtained in the fitting procedure (the experimental frequencies between 200 and 280 K, have not been used in the fit). Since most of the internal modes are not well frequency-isolated, the error bars on the frequency values are of order $\pm 1\ cm^{-1}$.

Two types of modes appear from these calculations. The first type includes the ν_1, ν_7, ν_9 and ν_{12} modes. In this case, coefficient b_i has a negative value and the critical exponent β_i is near 0.5: the average value of β_i for these four modes is 0.48 ± 0.06. These modes are driven by a linear pseudospin coupling with phonons. The ν_2, ν_3, ν_5 and ν_{11} modes belong to the second class, where $\beta_i > 0.5$ (the average value of β_i is 0.70 ± 0.08). The dominant coupling is quadratic for these modes.

These results can be interpreted in two slightly different ways. The linear coupling in pseudospins is the result of interactions between a disordered $(CH_3NH_3)^+$ cation and a neighbouring $(Bi_2Cl_{11})^{5-}$ anion. This process is reflected in the two NH_3 stretching, the asymmetric NH_3 bending and the NH_3 rocking modes. In this case, the short-range interactions (particularly the N–H $\cdots$ Cl hydrogen bonds between the two ions) are dominant and they are subject to important changes when the cation reorients. The quadratic coupling in pseudospins is due to the interactions between two disordered $(CH_3NH_3)^+$ cations. It is observed for the symmetric CH_3 stretching, the symmetric NH_3 bending, the C–N stretching and the CH_3 rocking modes. Long-range coulombic

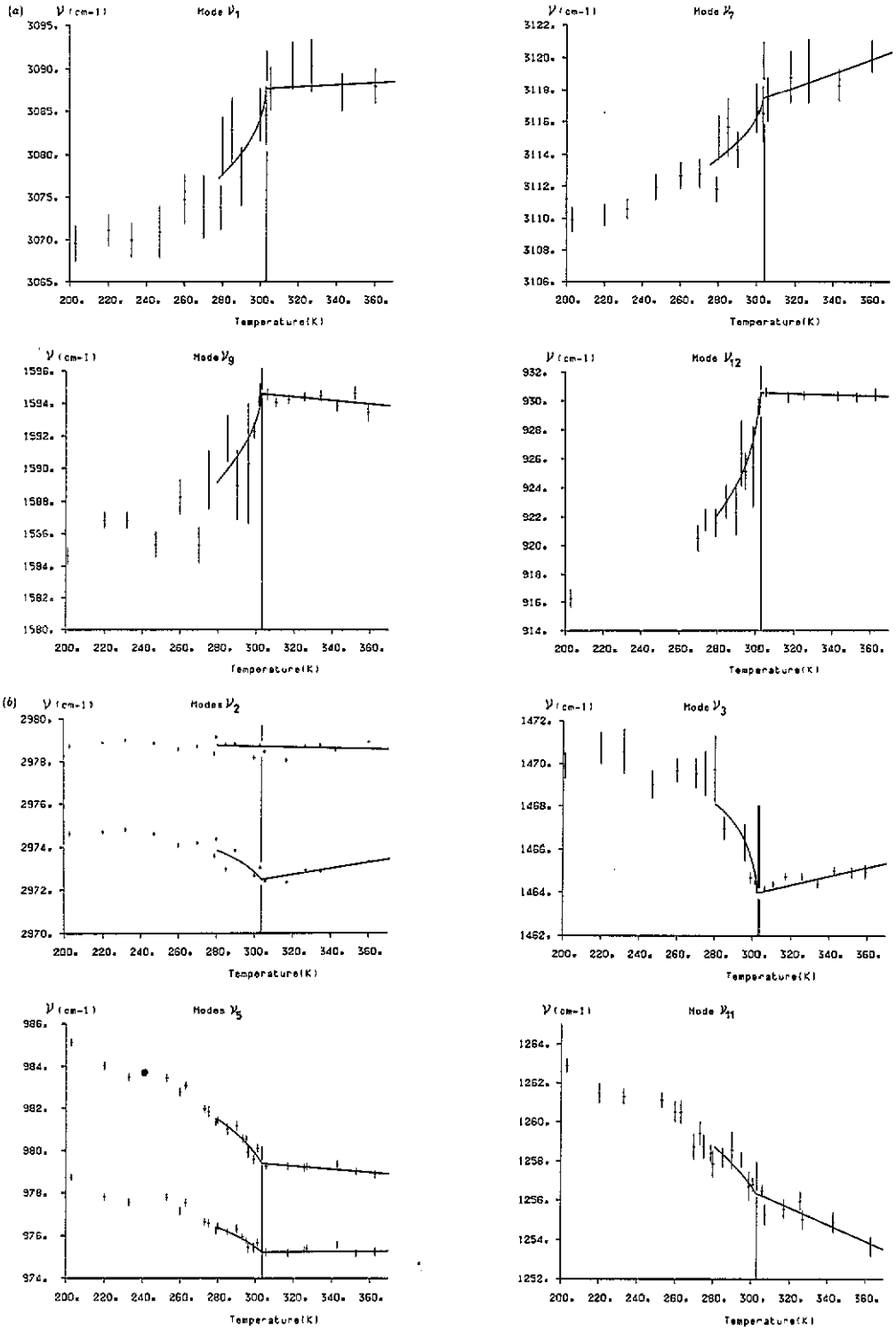

Figure 4. Temperature dependence of the internal mode frequencies of MAPCB. Experimental points are reported with their error bar. The full lines correspond to calculated frequencies using equation (16) between 280 and 360 K. (*a*) Modes with a linear pseudospin coupling to phonons (ν_1, ν_7, ν_9 and ν_{12} modes). (*b*) Modes with a quadratic pseudospin coupling to phonons (ν_2, ν_3, ν_5 and ν_{11} modes).

Table 4. The best sets of parameters used to adjust the experimental frequencies versus temperature.

Mode	$\omega_{0,i}$	a_i	b_i	β_i
ν_1	3084.5	−65.0	−15615.0	0.46 ± 0.23
ν_2	2968.5	−78.4	1568.0	0.58 ± 0.18
ν_3	1459.6	−44.8	1125.0	0.76 ± 0.11
ν_5*	975.2	−0.2	179.0	0.81 ± 0.09
	982.1	17.2	287.0	
ν_7	3104.7	−260.3	−4615.0	0.41 ± 0.32
ν_9	1598.1	37.3	−2822.0	0.60 ± 0.14
ν_{11}	1269.1	106.7	441.0	0.67 ± 0.12
ν_{12}	932.0	9.6	−3872.0	0.45 ± 0.06

* For ν_5, the two components have been fitted with a common critical exponent.

forces are responsible for the interactions between two disordered cations separated by about 10 Å. The value of the critical exponent, $\beta_i = 0.70$, may indicate the existence of correlations between two neighbouring cations.

6. Conclusion

The internal modes of the methylammonium cations of MAPCB have been assigned, in agreement with the results of other crystals containing $(CH_3NH_3)^+$ cations. As was concluded from the structural study [3], the observed position of the bands confirms the existence of hydrogen bonds in MAPCB. Owing to the different surroundings of the cations, most modes present a Davidov splitting. The overtones of the two CH_3 bending modes are coupled with the symmetric CH_3 stretching mode, as for methylammonium chloride [21]. These bands have been assigned unambiguously, with the help of the results from the partially deuterated compound.

In general, the frequency versus temperature curves of the observed modes around the phase transition T_{C_1} revealed three types of behaviour. A first possibility appears when frequency variation is observed between the paraelectric and the ferroelectric phases. Such modes correspond to the motions of ordered methylammonium cations like, for example, the highest component of the ν_2 mode (see figure 4). The second type of behaviour appears when the frequency increases with temperature and a change in the slope is observed at T_{C_1}. These frequency variations have been explained by a linear coupling of the pseudospins representing the disordered methylammonium cations with phonons. The third possibility corresponds to the lines whose frequency decreases with temperature, showing a change in slope at T_{C_1}. This last case is due to a quadratic coupling of the pseudospins with phonons.

This paper reports only a part of the dynamical properties of MAPCB. To interpret correctly the behaviour of the internal modes of the methylammonium cations near the II–III PT, the structure of the polar phase III should be known; x-ray diffraction measurements of this phase are now in progress. It is also of interest to continue the Raman scattering study of the lattice modes and the internal modes of the $(Bi_2Cl_{11})^{5-}$ anion.

Acknowledgments

One of us (RJ) is grateful to the French Ministry of Research and Technology for supporting his stay at Lille. The authors express sincere thanks to Dr A Mierzejewski for fruitful discussions and his reading of the manuscript.

References

[1] Jakubas R 1989 *Solid State Commun.* **69** 267
[2] Jakubas R, Sobczyk L and Lefebvre J 1989 *Ferroelectrics* **100** 143
[3] Lefebvre J, Carpentier P and Jakubas R 1991 *Acta Crystallogr.* B **47** 228
[4] Matuszewski J, Jakubas R, Sobczyk L and Głowiak T 1990 *Acta Crystallogr.* C **46** 1385
[5] Jakubas R and Sobczyk L 1989 *Ferroelectrics* **92** 365
[6] Cach R and Jakubas R 1990 *Ferroelectrics* **108** 121
[7] Mróz J, Poprawski R, Kolarz A and Jakubas R 1990 *Solid State Commun.* **76** 821
[8] Mróz J and Jakubas R 1989 *Solid State Commun.* **72** 813
[9] Mróz J and Jakubas R 1991 *Ferroelectrics* 118–29
[10] Iwata M and Ishibashi Y 1990 *J. Phys. Soc. Japan* **59** 4239
[11] Pawlaczyk C, Motsch H, Jakubas R and Unruh H-G 1990 *Ferroelectrics* **108** 127
[12] Jakubas R and Pykacz H 1989 *Phys. Status Solidi* a **115** K17
[13] Miniewicz A and Jakubas R 1991 *J. Mol. Electr.* **7** 55
[14] Miniewicz A and Jakubas R 1990 *J. Mol. Electr.* **6** 113
[15] Przesławski J, Kosturek B and Jakubas R 1991 *Izv. Akad. Nauk SSSR Ser. Fiz.* **55** 510
[16] Kosturek B and Jakubas R 1989 *Phys. Status Solidi* a **114** K111
[17] Piekara-Sady L, Jakubas R and Pislewski N 1989 *Solid State Commun.* **72** 587
[18] Jakubas R and Lefebvre J 1990 *Ferroelectrics* **108** 115
[19] Bhattacharjee R, Varma V, Fernandes J R and Rao C N R 1990 *Ferroelectrics Lett.* **12** 79
[20] Pawlaczyk C 1992 in preparation
[21] Meinander N, Bergström G, Forss S and Stenman F 1979 *J. Raman Spectrosc.* **8** 265
[22] Sundius T and Meinander N 1981 *J. Mol. Struct.* **76** 227
[23] Prasad P S R and Bist H D 1989 *J. Phys. Chem. Solids* **50** 1033
[24] Petzelt J and Dvořák V 1976 *J. Phys. C: Solid State Phys.* **9** 1571
[25] Petzelt J and Dvořák V 1976 *J. Phys. C: Solid State Phys.* **9** 1587
[26] Matsushita M 1976 *J. Chem. Phys.* **65** 23
[27] Winterfeldt V, Schaack G and Klöpperpieper A 1977 *Ferroelectrics* **15** 21
[28] Schaack G and Winterfeldt V 1977 *Ferroelectrics* **15** 35
[29] Bajpai P K, Jain Y S and Bist H D 1990 *J. Raman Spectr.* **21** 327
[30] Eliott R J 1971 *Light Scattering in Solids* ed M Balkanski (Paris: Flammarion) p 354
[31] Mróz J and Jakubas R 1990 *Ferroelectrics Lett.* **11** 53